HHS Public Access

Author manuscript

Free Radic Biol Med. Author manuscript; available in PMC 2021 January 01.

Published in final edited form as:

Free Radic Biol Med. 2020 January ; 146: 324–332. doi:10.1016/j.freeradbiomed.2019.11.016.

The thiocyanate analog selenocyanate is a more potent antimicrobial pro-drug that also is selectively detoxified by the host

Brian J. Day[1,3,4,*], **Preston E. Bratcher**[2], **Joshua D. Chandler**[5,6], **Matthew B. Kilgore**[5,6], **Elysia Min**[1], **John J. LiPuma**[7], **Robert J. Hondal**[8], **David P. Nichols**[9]

[1]Department of Medicine, National Jewish Health, Denver, CO 80206

[2]Department of Pediatrics, National Jewish Health, Denver, CO 80206

[3]Department of Medicine University of Colorado, Aurora, CO 80045

[4]Department of Pharmaceutical Sciences, University of Colorado, Aurora, CO 80045

[5]Department of Pediatrics, Emory University, Atlanta, GA 30322

[6]Center for CF and Airways Disease Research, Children's Healthcare of Atlanta, Atlanta, GA 30322

[7]Department of Pediatrics, University of Michigan, Ann Arbor, MI 48109

[8]Department of Biochemistry, University of Vermont, Burlington, VT 05405

[9]Department of Pediatrics, University of Washington, Seattle, WA 98195.

Abstract

A hallmark of cystic fibrosis (CF) lung pathology is an increased susceptibility to pulmonary infections. Thiocyanate ($^{-}$SCN) is an endogenous component of the innate immunity's peroxidase system that converts $^{-}$SCN to the antimicrobial agent hypothiocyanite (HOSCN). We have previously shown that the host thioredoxin reductase (TrxR), but not the pathogen's TrxR, can selectively detoxify HOSCN thereby decreasing inflammation and oxidative stress. We tested whether the $^{-}$SCN analog selenocyanate ($^{-}$SeCN) shares these properties against several clinical CF bacterial isolates. We examined oxidant production from a lactoperoxidase (LPO) system using $^{-}$SeCN as a potential substrate. The LPO system generated an oxidant similar in nature to HOSCN and consistent with being HOSeCN. The rate of oxidant generation using $^{-}$SeCN was significantly less than seen for $^{-}$SCN. An LPO system was used to generate HOSCN or HOSeCN and compared for antimicrobial activity during *in situ* exposure of clinical CF isolates of *P. aeruginosa* (PA), *B. cepacia* complex (BCC), and methicillin-resistant *S. aureus* (MRSA) obtained from CF sputum samples. Bacterial viability was assessed by colony forming units. Selective detoxification

[*]To whom correspondence should be addressed: Brian J Day: Department of Medicine, National Jewish Health, Denver CO 80206; dayb@njhealth.org; Tel. (303) 398-1121; Fax. (303) 270-2263.

of HOSeCN was determined by comparing its metabolism by mammalian thioredoxin reductase (TrxR) to bacterial TrxR following the consumption of NADPH. We also assessed potential toxicity of equivalent HOSeCN generation, which demonstrated *in situ* antimicrobial activity, in human bronchial epithelial cells with a cell viability assay. The ⁻SeCN/HOSeCN system was much more potent than ⁻SCN/HOSCN system at killing PA, BCC and MRSA isolates. The ⁻SeCN/HOSeCN system was more effective at killing ⁻SCN/HOSCN resistant isolates. Mammalian TrxR selectively detoxified HOSeCN whereas the bacterial TrxR enzyme showed little activity. Human bronchial epithelial cells exposed to equivalent flux of HOSeCN that killed several CF pathogens showed no decrease in viability. ⁻SeCN may be an effective therapeutic for the treatment of CF lung pathogens that are difficult to treat with current antibiotics.

Graphical Abstract

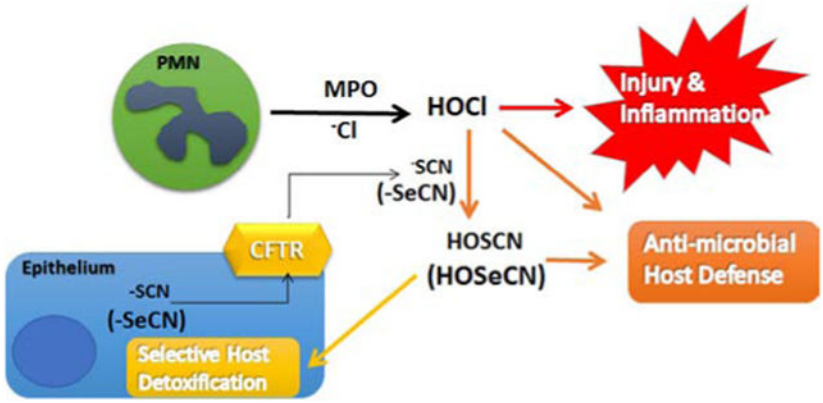

Keywords

haloperoxidases; hypohalous acids; innate immunity; host defense; antimicrobials; cystic fibrosis; Pseudomonas aeruginosa; Burkholderia cepacia complex; Staphylococcus aureus

Introduction

Cystic fibrosis (CF) is a genetic disorder due to loss of function mutations in the cystic fibrosis transmembrane conductance regulator (CFTR) protein (1). CF is characterized by persistent lung infection with common bacteria including *Pseudomonas aeruginosa* (PA), *Burkholderia cepacia complex* (BCC), and methicillin-resistant *Staphylococcus aureus* (MRSA) (2). These pathogens frequently develop broad antibiotic resistance over the course of clinical care. A direct role for the mutant CFTR protein in the impairment of lung innate immunity is not known. CFTR protein regulates apical anion transport across epithelial cells (3-6). Among the endogenous anions that passivate through the CFTR channel are halides and pseudohalide such as chloride and thiocyanate (⁻SCN) (7).

⁻SCN is generated by the detoxification of cyanide and known to originate from the diet and environmental factors, with a mean plasma concentration in humans of 20-50 μM (12). ⁻SCN is concentrated in human saliva at 830 μM (14), as well as nasal fluid at 400 μM (13) and in sheep airway lining fluid at 160 μM (15). The CFTR protein is an important

transporter of $^{-}$SCN, which has been demonstrated to be decreased in apical secretions from CF airway epithelial cells (4), CF animal model secretions (16), and human CF saliva (17). Higher $^{-}$SCN levels correlate with better lung function in patients with CF (13). $^{-}$SCN is oxidized to HOSCN by haloperoxidases (e.g., myeloperoxidase (MPO), lactoperoxidase (LPO)) (9) that reside in neutrophils (MPO) and in the airway lining fluid (LPO). HOSCN is a selective oxidant preferring low pK_a thiols and selenols (RSH and RSeH) (18) and is used by the immune system to kill bacteria (11), fungi (19) and viruses (20, 21). We have previously shown that mammalian selenocysteine (Sec)-containing thioredoxin reductase (Sec-TrxR) can metabolize HOSCN in human lung epithelia (22). The bacterial form of TrxR lacks selenocysteine and cannot metabolize HOSCN and instead is inactivated by HOSCN (22).

Selenocyanate ($^{-}$SeCN) is a chemical analog of endogenous $^{-}$SCN. Substitution of selenium for sulfur in a compound usually results in a more chemically reactive compound (23). We hypothesized that $^{-}$SeCN is treated by the body in a similar manner as $^{-}$SCN and will be converted by haloperoxidases to a more potent antimicrobial oxidant, presumably hyposelenocyanite (HOSeCN), while keeping its ability to be selectively detoxified by the host Sec-TrxR.

Materials and Methods

Sources of Purified Enzymes

Recombinant mouse mitochondrial thioredoxin reductase (Sec-TrxR2) was produced from semisynthesis as described previously (24). Recombinant thioredoxin reductase (Cys-TrxR) and thioredoxin (Trx) from *E. coli* was purchased from Cayman-IMCO. Bovine milk lactoperoxidase (LPO), glucose oxidase (GOX) from *Aspergillus*, and catalase from bovine liver were purchased from Sigma.

Generation of HOSCN and $^{-}$SeCN-derived oxidant

KSeCN and NaSCN were purchased from Sigma-Aldrich. HOSCN and $^{-}$SeCN-derived oxidant were generated as described previously with modifications (25). Briefly, reaction solutions contained bovine LPO (38.7 nM), $^{-}$SeCN (1 mM) or $^{-}$SCN (1 mM), glucose (6 mM), and increasing amounts of glucose oxidase (GOX). Reactions were stopped by addition of catalase (1000 U/ml). HOSCN or the $^{-}$SeCN-derived oxidant concentrations were determined as described below. For kinetic studies, reactions were carried out in Eppendorf tubes and time points taken for HOSCN or $^{-}$SeCN-derived oxidant determinations using a double beam spectrophometer (UV-2501PC, Shimadzu, Kyoto, Japan). For bulk generation of HOSCN or the $^{-}$SeCN-derived oxidant the following procedure was used, briefly, 6.5 mM of NaSCN or KSeCN and 60 units/mL LPO were prepared in 10 mM PBS, pH 7.4, then pulsed with approximately 1 mM (final) hydrogen peroxide seven times over an equal number of minutes (for LC-MS experiments, LPO concentration was 12 U/ml and PBS pH was 6.7). After 7 minutes, 1000 units/mL catalase was added to remove excess peroxide. The solution was centrifuged at 14,000 × g for 5 minutes at 4°C in a 10-kDa cutoff filter to remove proteins and diluted in a known concentration of 2-nitro-5-thiobenzoate ($^{-}$NTB). HOSCN or the $^{-}$SeCN-derived oxidant

concentrations were determined by formation of 5,5'-dithiobis(2-nitrobenzoic acid (DNTB) and the loss of signal at A_{412} (ε = 14,150 M^{-1} cm^{-1}) (26). This procedure yielded 1-2 mM HOSCN or the $^{-}$SeCN-derived oxidant that was stable on ice for at least 15 minutes.

Detection of HOSCN and $^{-}$SeCN-derived oxidant by HPLC

HOSCN and $^{-}$SeCN-derived oxidant was detected using HPLC with electrochemical detection. Using reversed-phase chromatography with 5mM tetrabutylammonium bisulfate as an ion-pairing agent in a mobile phase containing 3% acetonitrile at pH 7, oxidation products of $^{-}$SCN and $^{-}$SeCN were detected and separated. Electrochemical potentials at 500 mV and 1600 mV were applied to identify the peaks, using a CoulArray electrochemical detector (ESA) attached in series to a boron-doped diamond (BDD) electrode (ESA). 10 μL of the sample was injected into a system with a flow rate of 1 mL/min and the column at 27°C. Under these conditions, HOSCN elutes at 3.25 min, $^{-}$SCN elutes at 6.05 min, $^{-}$SeCN-derived oxidant elutes at 6.46 min, and $^{-}$SeCN elutes at 9.93 min.

HOSCN or the $^{-}$SeCN-derived oxidant identification by mass spectrum analysis

HOSCN or the $^{-}$SeCN-derived oxidant were generated and quantified as described above, then diluted to 10 μM in PBS. Negative controls were matched samples that had not been treated with hydrogen peroxide, and were diluted by the same factor as the oxidant-containing samples. The samples were extracted with two volumes of ice-cold LC-MS grade acetonitrile (MillporeSigma, St. Louis, MO, USA) with brief vortexing and 30 minutes incubation on ice before centrifugation at 20,627 *g* at 4 °C for 10 min. The extracts were then transferred to autosampler vials and held at 4 °C prior to injection and liquid chromatography of 2.5 μl sample injected into a SeQuant ZIC-HILIC 150 × 2.1 mm column with 3.5 μm particle size and 100 angstrom pore size, and a 20 × 2.1 mm matching guard column (MillporeSigma, Burlington, MA, USA). Mobile phases were LC-MS grade water (Phase A) or acetonitrile (Phase B) with 0.1% formic acid run at a flow rate of 0.25 ml/min and a column temperature of 40 °C. Each run started with equilibration at 10% A for 8.3 minutes. A 17.5 minute gradient from 10% to 80% A began concurrent with sample injection (2.5 μl), followed by a 7.5-minute hold. Eluate was introduced to a Q Exactive HF (Thermo, Waltham, MA, USA) mass spectrometer via a HESI-II source held at −2.7 kV. In some experiments the initial volume corresponding to column void was diverted to waste (up to 1.56 min). Quadrupole scanning was set to 50-500 *m/z* with AGC target of 1e6, a maximum injection time of 200 ms, and an Orbitrap resolving power of 120,000. Intensity data were extracted from Xcalibur v. 4.1 (Thermo, Waltham, MA, USA) using a 5 ppm mass accuracy window for all ions and graphed in R v. 3.5.3 using 'ggplot2' package version 3.0.

Hydrogen peroxide assay

Hydrogen peroxide was measured using a calibrated hydrogen peroxide electrode connected to a free radical analyzer (WPI, Sarasota, FL). Briefly, reactions with glucose (6 mM) and increasing concentrations of glucose oxidase (GOX, 10-100 mU/mL) in PBS were incubated for 2 hours at room temperature to determine GOX generation of hydrogen peroxide. Separate reactions containing GOX plus the full peroxidase system (LPO 38.7 nM) with $^{-}$SCN (1mM) or $^{-}$SeCN (1mM) were also incubated at room temperature for 2 hours to determine residual hydrogen peroxide leftover from peroxidase reaction. Hydrogen peroxide

electrode was calibrated with a 6-point hydrogen peroxide standard curve. Hydrogen peroxide concentrations of standards were determined using extinction coefficient A_{240} = 43.6 M^{-1} cm^{-1} (27) and data was plotted as the mean of two replicates.

HOSCN and HOSeCN Oxidoreductase Assay

Reaction mixture contained 75 nM mammalian Sec-TrxR2 or bacterial Cys-TrxR and 200 μM NADPH in PBS at room temperature. Reactions were started with addition of HOSCN or HOSeCN. Baseline rates without enzyme were subtracted from total activity. Activity was based on change in NADPH A_{340} (ε= 6220 M^{-1} cm^{-1}) (28).

Enzyme Kinetics

Oxidoreductase activity *in vitro* was fit to the Michaelis-Menten kinetic equation: Y = V_{max}[S]/(K*m* + [S]). Data were fit using least squares method with Prizm 5 Software (GraphPad).

Mammalian Cell Culture

Human bronchial epithelial cells (16HBE14o-) were maintained in DMEM supplemented with FBS (Cellgro), 100 nM methylselenocysteine (Sigma), and penicillin-streptomycin (Cellgro). Cells were grown in submerged conditions to approximately 85% confluence in 24-well plates (Falcon). Cell viability was determined by the lactate dehydrogenase (LDH) assay 24 hours after the beginning of exposure as described previously (29).

Bacterial Strains and Culture

Most bacterial isolates were obtained from the National Jewish Clinical Laboratory that were originally isolated from sputum samples obtained from individuals with cystic fibrosis. Some BCC cystic fibrosis clinical isolates were obtained from Dr. LiPuma's CF repository (University of Michigan). All bacteria species were identified or identities confirmed using MALDI Biotyper (Bruker). All clinical isolates were de-identified prior to use. Bacterial isolates were maintained in lysogeny broth (LB). For cell viability assay, bacteria were diluted to 1 × 10^6 cfu/mL for treatment and then serially diluted from 1:100 to 1:10,000 and plated on LB agar. Colonies were counted following overnight incubation at 37°C to determine viability.

Oxidase-Peroxidase-coupled System

Mammalian and bacterial cells were exposed to an inflammation-mimicking enzyme system containing 6 mM glucose, 3 mU/mL of glucose oxidase, 5 units/mL LPO and 400 μM $^-$SeCN or 400 μM $^-$SCN in PBS, pH 7.4, for 2 hour before returning to full medium (16HBE14o-) or plated on LB agar (bacteria).

Bacterial HOSCN and HOSeCN IC_{50} assay

Assays were performed with 1 × 10^6 bacteria incubated for 2 hours with LPO/glucose oxidase (GOX)/$^-$SCN or $^-$SeCN system that generates increasing levels of either HOSCN or HOSeCN (HOX) by raising the GOX levels as determined by standard curves. HOX generation rates were estimated based on kinetics obtained in Figure 3. Bacteria were plated

on agar plates and incubated at 37°C for 1-2 days. Colony forming units (CFU) were determined by dilution method. CFUs were converted to % viability and data curves fitted using nonlinear regression (Log [HOX flux] vs normalized response – variable slope) and least squares method for best fit. IC_{50} and 95% confidence intervals were determined from the generated data curves (Prizm 5 GraphPad software).

Statistics

Graphical data are expressed as means ± S.E. Prism 5 (GraphPad) was used to perform and evaluate one-way analysis of variances with Tukey's post-test. A p value of $p<0.05$ was considered significant.

RESULTS

We investigated whether a lactoperoxidase (LPO) system could use $^{-}$SeCN as a substrate to generate an oxidant similar to HOSCN (Figure 1). Samples were incubated with bovine milk LPO (60 U/ml), $^{-}$SeCN (6.5 mM) or $^{-}$SCN (6.5 mM), and pulsed 7 times with hydrogen peroxide (1 mM) required to activate LPO. Loss of $^{-}$SCN and $^{-}$SeCN and the formation of HOSCN and $^{-}$SeCN-derived oxidant were examined by HPLC with electrochemical detection. $^{-}$SCN had a shorter retention time than $^{-}$SeCN with $^{-}$SCN eluting at 6 minutes compared to $^{-}$SeCN eluting at 10 minutes with electrode potential set at 1600 mV (Figure 1). $^{-}$SeCN has a lower redox potential than $^{-}$SCN where some of the signal occurs at 500 mV with $^{-}$SeCN. Upon incubation with the LPO system, both $^{-}$SCN and $^{-}$SeCN levels dropped with the formation of a new peaks detected at a lower electrode potential of 500 mV. HOSCN peak eluted at 3.5 minutes compared with $^{-}$SeCN-derived oxidant which eluted at 6.5 minutes.

To better confirm the oxidant derived from using $^{-}$SeCN as a substrate in the LPO system, we analyzed 10 μM of each of the oxidants formed by the LPO system by liquid chromatography-mass spectrometry, as well as negative controls for each electron donor without the addition of hydrogen peroxide (Figure 2). We extracted ions matching to the $[M-H]^{-}$ ions of HSCN, HOSCN, HSeCN and HOSeCN with 5 ppm mass accuracy. As expected, $^{-}$SCN-LPO without hydrogen peroxide gave a peak of 57.9755 *m/z* (−3.4 ppm) and 4.1 min (Figure 2A), while adding hydrogen peroxide produced the expected oxidant HOSCN with a peak of 73.9705 *m/z* (−1.4 ppm) and 1.8 min (Figure 2B), with a relative decrease in the intensity of the $^{-}$SCN peak. $^{-}$SeCN also produced a strong $[M-H]^{-}$ ion of 105.9200 *m/z* (−1.9 ppm) at 3.5 min; Figure 2C), and when hydrogen peroxide was added a second peak of the same *m/z* was_observed at 1.7 min, similar to the retention time of HOSCN (Figure 2D). The 3.5 min $^{-}$SeCN peak also decreased in intensity when hydrogen peroxide was added. Finally, low ($<10^5$) intensity ions corresponding to HOSeCN (121.9149 *m/z*, −1.6 ppm) and HOSCN co-eluted with peaks of $^{-}$SeCN and $^{-}$SCN, respectively (data not shown); this supports the notion that $^{-}$SeCN can bond with a single atom of oxygen, like $^{-}$SCN. Taken together, the LC-MS data suggest that the $^{-}$SeCN-derived oxidant was reduced back to $^{-}$SeCN at the electrospray ionization source but not before then, which allowed its chromatographic separation from reduced $^{-}$SeCN. To consider selenocyanogen ($SeCN_2$) as possible alternative for the identity of the oxidant we looked for the expected $[M-H]^{-}$ *m/z* of

210.8319 but did not observe even trace amounts of this. Because the retention time of the $^{-}$SeCN-derived oxidant is very similar to that of HOSCN, and both $^{-}$SCN and $^{-}$SeCN exhibited similar in-source oxidation with a single atom of oxygen, the data are consistent with this oxidant likely being HOSeCN. Both HOSCN and the $^{-}$SeCN-derived oxidant are not stable and decay to undetectable levels after 24 hours (data not shown). This is the first reported evidence that LPO can use $^{-}$SeCN as a substrate to generate an oxidant consistent with being HOSeCN.

Quantitation of both HOSeCN and HOSCN was measured over 2 minutes using their ability to oxidize 2-nitro-5-thiobenzoate ($^{-}$NTB) to 5, 5'-dithiobis(2-nitrobenzoic acid) DNTB (Figure 3). The rate of HOSCN formation in the LPO system was 103 ± 3 nM/min/GOX mU/mL. The rate of HOSeCN formation in the LPO system was 13.5 ± 0.8 nM/min/GOX mU/mL. There was no observed formation of HOSCN in the absence of LPO whereas there was a small rate (0.5 ± 0.05 nM/min/GOX mU/mL) of HOSeCN produced in the absence of LPO. The overall generation of HOSeCN from the LPO system was much less than that observed for HOSCN with $^{-}$SCN as a substrate. It is interesting to note that $^{-}$SeCN, but not $^{-}$SCN, can directly react with hydrogen peroxide to form HOSeCN, but only at high hydrogen peroxide levels and at much slower rates. These concentrations of hydrogen peroxide and slow rate of formation are not likely physiologically relevant. Rates of oxidants produced by LPO were used to estimate the oxidant formation in antimicrobial activities of $^{-}$SCN and $^{-}$SeCN. Most of the hydrogen peroxide generated by GOX is consumed by LPO generation of both HOSCN and HOSeCN over a 2-hour incubation (Figure 4). There is more hydrogen peroxide consumption with $^{-}$SeCN plus the LPO system than seen with $^{-}$SCN with the LPO system. This may be due to the ability of $^{-}$SeCN to directly react with hydrogen peroxide.

Previously our group has shown that HOSCN could be metabolized by mammalian thioredoxin reductase (22). We examine whether HOSeCN could also be metabolized by mammalian selenocysteine (Sec)-containing thioredoxin reductase (Sec-TrxR) as compared with bacterial cysteine (Cys)-containing thioredoxin reductase (Cys-TrxR). Purified recombinant mouse mitochondrial Sec-TrxR2 and bacterial Cys-TrxR from *E. coli* were used to determine their ability to catalytically metabolize HOSeCN by following loss of NADPH over time (Figure 5). Baseline controls were run to assess any direct reaction of HOSeCN with NADPH and this background was subtracted from the total to obtain enzymatic activity. Kinetic analysis revealed a typical Sec-TrxR enzymatic saturation curve with a V_{max} of 12 ± 1 μM/min, k_{cat} of 161 ± 17 min^{-1} and a K_M of 33 ± 7 μM for HOSeCN. The Sec-TrxR approximate second order rate constant for HOSeCN was 8.1×10^4 M^{-1} s^{-1}. These values are similar but lower than those we previously reported for HOSCN (22). The bacterial form of Cys-TrxR had detectable enzymatic activity for HOSeCN only at higher (>30 μM) concentrations.

HOSCN was previously shown to be a potent inhibitor of bacterial Cys-TrxR (22). We examined whether HOSeCN could also inhibit Cys-TrxR activity. Cys-TrxR from *E. coli* was incubated for 5 minutes in the presence of NADPH and increasing concentration of either HOSCN or HOSeCN and then assayed for the ability to reduce DNTB in a thioredoxin-dependent manner. Both HOSCN and HOSeCN inhibited Cys-TrxR in a dose-

dependent manner (Figure 6). HOSeCN was slightly more potent inhibitor with a calculated IC_{50} of 4.3 μM and a 95% confidence interval of 3.3 – 5.6 μM whereas HOSCN had a calculated IC_{50} of 9.3 μM and a 95% confidence interval of 8.6 – 10.1 μM.

We assessed whether there would be any differential cytotoxicity for HOSeCN between host and pathogen. Human bronchial epithelial cells (16HBE) and CF clinical isolates of *Pseudomonas aeruginosa, Burkholderia mutlivorans* and methicillin resistant *Staphylococcus aureus* (MRSA) were exposed for 2 hours with the LPO system generated HOSeCN at pH 7.4 and then media was replaced and cell viability was assessed 24 hours after exposure (Figure 7). Under these conditions, residual hydrogen peroxide levels generated by the GOX system as determined in Figure 4 were not cytotoxic to either the bronchial epithelial cells or the bacteria (data not shown). In fact, residue hydrogen peroxide levels (GOX 3mU/ml) under the conditions used to generate HOSeCN were not detectable by the hydrogen peroxide electrode. $^{-}$SeCN at 400 μM was also not toxic by itself to bronchial epithelial cells or the bacteria. We observed a reduction in pathogen viability without any observable cytotoxicity to host epithelial cells to HOSeCN generated by the full LPO system. The *Burkholderia cepacia* complex in general appears to be less sensitive to HOSeCN cytotoxicity than *Pseudomonas aeruginosa* and methicillin-resistant Staphylococcus aurous clinical isolates tested.

One potential issue with HOSCN as an antimicrobial agent is resistance in bacteria isolates associated with CF lung infections. We screened fifteen bacterial isolates consisting of *Burkholdria cepacia* complex (BCC), *Pseudomonas aeruginosa* (PA) and methicillin-resistant *Staphylococcus aureus* (MRSA) for resistance to HOSCN (Table 1). CF clinical bacteria isolates were incubated for 2 hours with a $^{-}$SCN/LPO system that generates increasing levels of HOSCN. After HOSCN exposure, bacteria are returned to growth media and plated to assess viability by colony forming units. The HOSCN generation that inhibits viability by 50% (IC_{50}) was determined by curve fitting the data. We have observed HOSCN-resistant CF clinical isolates of BCC, PA and MRSA (Figure 8). A HOSCN-sensitive CF clinical isolate of BCC (*B. multivorans*) exhibited an IC_{50} toward HOSCN flux of 68 μM/hr (95% CI: 52-91 μM/hr) whereas a resistant BCC isolate (*B. dolosa*) had an IC_{50} of 202 μM/hr (95% CI: 167-245 μM/hr) HOSCN flux (Figure 8A). A $^{-}$SCN-sensitive CF clinical isolate of PA (PA-39) exhibited an IC_{50} toward HOSCN flux of 13 μM/hr (95% CI: 10-18 μM/hr) whereas a resistant PA isolate (PA-T) had an IC_{50} of 124 μM/hr (95% CI: 96-161 μM/hr) HOSCN flux (Figure 8B). It is interesting to note that the PA-T isolate was also found to be tobramycin resistant. We observed the widest range of $^{-}$SCN resistance in CF clinical isolates of MRSA. A $^{-}$SCN-sensitive CF clinical isolate of MSRA (MRSA-46) exhibited an IC_{50} toward HOSCN flux of 25 μM/hr (95% CI: 19-34 μM/hr) whereas a resistant MRSA isolate (MRSA-43) had an IC_{50} around 1,591 μM/hr (95% CI: 201-12,618 μM/hr) (Figure 8C).

We examined whether $^{-}$SeCN would be more potent than $^{-}$SCN against common CF lung pathogens in both $^{-}$SCN sensitive and resistant CF clinical isolates. We found that $^{-}$SeCN was a more potent antimicrobial pro-drug than $^{-}$SCN in both $^{-}$SCN-sensitive and resistant CF clinical isolates (Figure 9). In a $^{-}$SCN-sensitive BCC clinical isolate (*B. multivorans*), we observed an IC_{50} toward HOSCN flux of 68 μM/hr compared to only 2 μM/hr flux (95% CI:

1.7-3.1 μM/hr) for HOSeCN (Figure 9A). A similar effect was seen in the $^{-}$SCN-resistant BCC isolate (*B. vietnamiensis*) where an IC_{50} toward HOSCN flux of 167 μM/hr was observed compared with only 6 μM/hr flux (95% CI: 4.1-8.1 μM/hr) for HOSeCN (Figure 9B). In a $^{-}$SCN-sensitive PA clinical isolate (PA-39), we observed an IC_{50} toward HOSCN flux of 13 μM/hr compared to only 2 μM/hr flux (95% CI: 1.3-2.4 μM/hr) for HOSeCN (Figure 9C). A similar effect was seen in the $^{-}$SCN-resistant PA isolate (PA-T) where an IC_{50} toward HOSCN flux of 124 μM/hr was observed compared with only 3 μM/hr flux (95% CI: 2.0-4.3 μM/hr) for HOSeCN (Figure 9D). In the $^{-}$SCN-sensitive MRSA clinical isolate (MRSA-46), we observed an IC_{50} towards HOSCN flux of 25 μM/hr compared to 1 μM/hr flux (95% CI: 0.6-1.3 μM/hr) for HOSeCN (Figure 9E). However, in a $^{-}$SCN-resistant MRSA (MRSA-43) we were not able to obtain an accurate IC_{50} (~1591 μM/hr) for HOSCN but were able to kill this resistant isolate with HOSeCN with an IC_{50} of 11 μM/hr (95% CI: 5.5-20.2 μM/hr) (Figure 9F).

DISCUSSION

Our previous studies have identified the unique properties of the $^{-}$SCN/haloperoxidase system that allow the host to generate the biocide HOSCN, which can be selectively detoxified by the host selenocysteine-containing thioredoxin reductase (Sec-TrxR) (22). We have identified some CF bacterial clinical isolates that are more resistant to the endogenous $^{-}$SCN/HOSCN peroxidase system and examined whether $^{-}$SeCN, a close chemical analog of $^{-}$SCN, would share many of the desirable properties of $^{-}$SCN with enhanced antimicrobial activity. Our studies revealed that $^{-}$SeCN behaves similarly to $^{-}$SCN where it is a substrate for the haloperoxidase system and generates a biocide that can be selectively metabolized by host Sec-TrxR but not bacterial Cys-TrxR. In addition, generating $^{-}$SeCN-derived oxidant at levels that kill bacteria does not affect lung epithelial cell viability. Furthermore, the $^{-}$SeCN/haloperoxidase system effectively kills a number of common cystic fibrosis lung pathogens, including those that are resistant to the $^{-}$SCN/haloperoxidase system.

We have made a novel discovery that selenocyanate ($^{-}$SeCN), a chemical analog of thiocyanate ($^{-}$SCN), can be utilized as a substrate by the lactoperoxidase (LPO) system and is converted to $^{-}$SeCN-derived oxidant, consistent with being HOSeCN. Haloperoxidases are extremely permissive enzymes that can metabolize a wide range of substrates beside the more commonly studied halides and pseudohalides (30). The rate and production of $^{-}$SeCN-derived oxidant was much lower than that seen for HOSCN and suggests that $^{-}$SeCN may have a lower turnover rate than $^{-}$SCN with LPO. Haloperoxidases can have different specificities and turnover rate for different substrates. For example, myeloperoxidase is the only haloperoxidase that can effectively utilize chloride as a substrate (31). However, it has a lower K_M and higher V_{max} for $^{-}$SCN than chloride (32). Haloperoxidase enzyme kinetics can be complex due to their ability to perform both one and two electron oxidations (31). More detailed enzyme kinetics will be needed to better understand this difference between $^{-}$SCN and $^{-}$SeCN as haloperoxidase substrates.

The $^{-}$SeCN-derived oxidant can be selectively metabolized by host Sec-TrxR but not by bacterial Cys-TrxR. It appears that HOSeCN is less readily metabolized by Sec-TrxR than HOSCN which we earlier reported a higher V_{max} and k_{cat} but similar K_M (22). This may be

due to HOSeCN being a stronger oxidant than HOSCN, resulting in more inactivation of the enzyme. However, this lower catalytic turnover of HOSeCN did not affect the ability for host cells to tolerate it compared to bacteria. It is likely that its property of being a better electrophile compared to HOSCN improves its potency as an antimicrobial agent. The HOSeCN was not an effective substrate for the bacterial Cys-TrxR as we have previously shown for HOSCN (22). TrxR is an important enzyme that provides reducing equivalents through thioredoxin that many enzymes rely on for catalytic activity (33). These include the peroxiredoxins (34) and ribonucleotide reductase (35). Ribonucleotide reductase is essential for life because it catalyzes the production of deoxyribonucleotides needed for DNA synthesis and repair (36). It is likely that ribonucleotide reductase is one of the bacterial targets of HOSeCN that contributes to its antimicrobial actions. Human lung epithelial cells tolerate HOSeCN much better than CF relevant pathogenic bacteria. We have found a number of clinical CF bacterial isolates with some resistance towards the $^{-}$SCN/LPO generating system suggesting that bacteria have developed defense mechanisms to deal with HOSCN. In fact, it has been speculated that commensal bacteria have HOSCN oxidoreductases that allow them to survive in saliva, which has some of the highest levels of HOSCN generation in the body (37).

HOSeCN is much better at killing CF relevant bacteria than HOSCN and readily kills $^{-}$SCN-resistant bacteria. We have found CF clinical isolates of *Burkholderia cepacia* complex, *Pseudomonas aeruginosa* and *Staphylococcus aureus* having increased resistance towards the HOSCN generating system. It is interesting that in each of these cases, the $^{-}$SeCN/LPO system also had lower IC_{50} values than the $^{-}$SCN/LPO system for the HOSCN-sensitive isolates. HOSCN is very specific towards proteins with cysteine groups having a low pK_a (38). HOSeCN is a stronger oxidant (electrophile) and likely has a broader range of cellular macromolecules it can target besides low pKa thiols. The increased reactivity of the HOSeCN may help eliminate these types of defenses in HOSCN-resistant bacteria.

This study found that $^{-}$SeCN can act as a biomimetic for thiocyanate by the body's host defense system that uses haloperoxidases to generate antimicrobial oxidants. $^{-}$SeCN's antimicrobial oxidant was found to effectively kill CF relevant bacteria and even those clinical isolates resistant to HOSCN. $^{-}$SeCN may be a more potent pro-drug than thiocyanate to treat CF lung infections.

Acknowledgements

This work was supported by a Cystic Fibrosis Foundation Research Grant (BJD and DPN) and NIH R01 HL14146 (BJD and RJH).

REFERENCES

1. Riordan JR, Rommens JM, Kerem B, Alon N, Rozmahel R, Grzelczak Z, et al. Identification of the cystic fibrosis gene: cloning and characterization of complementary DNA. Science. 1989;245(4922):1066–73. [PubMed: 2475911]
2. Lyczak JB, Cannon CL, Pier GB. Lung infections associated with cystic fibrosis. Clin Microbiol Rev. 2002;15(2):194–222. [PubMed: 11932230]
3. Quinton PM. Chloride impermeability in cystic fibrosis. Nature. 1983;301(5899):421–2. [PubMed: 6823316]

4. Fragoso MA, Fernandez V, Forteza R, Randell SH, Salathe M, Conner GE. Transcellular thiocyanate transport by human airway epithelia. J Physiol. 2004;561(Pt 1):183–94. [PubMed: 15345749]
5. Tang L, Fatehi M, Linsdell P. Mechanism of direct bicarbonate transport by the CFTR anion channel. J Cyst Fibros. 2009;8(2):115–21. [PubMed: 19019741]
6. Linsdell P, Hanrahan JW. Glutathione permeability of CFTR. Am J Physiol. 1998;275(1 Pt 1):C323–6. [PubMed: 9688865]
7. Linsdell P Thiocyanate as a probe of the cystic fibrosis transmembrane conductance regulator chloride channel pore. Can J Physiol Pharmacol. 2001;79(7):573–9. [PubMed: 11478590]
8. Ashby MT. Inorganic chemistry of defensive peroxidases in the human oral cavity. J Dent Res. 2008;87(10):900–14. [PubMed: 18809743]
9. Klebanoff SJ, Clem WH, Luebke RG. The peroxidase-thiocyanate-hydrogen peroxide antimicrobial system. Biochim Biophys Acta. 1966;117(1):63–72. [PubMed: 4380562]
10. Thomas EL, Fishman M. Oxidation of chloride and thiocyanate by isolated leukocytes. J Biol Chem. 1986;261(21):9694–702. [PubMed: 3015901]
11. Thomas EL, Milligan TW, Joyner RE, Jefferson MM. Antibacterial activity of hydrogen peroxide and the lactoperoxidase-hydrogen peroxide-thiocyanate system against oral streptococci. Infect Immun. 1994;62(2):529–35. [PubMed: 8300211]
12. Stoa KF. Determination of thiocyanate in serum with the pyridine-benzidine reaction. Scand J Clin Lab Invest. 1955;7(3):264–70. [PubMed: 13298606]
13. Lorentzen D, Durairaj L, Pezzulo AA, Nakano Y, Launspach J, Stoltz DA, et al. Concentration of the antibacterial precursor thiocyanate in cystic fibrosis airway secretions. Free Radic Biol Med. 2011;50(9):1144–50. [PubMed: 21334431]
14. Schultz CP, Ahmed MK, Dawes C, Mantsch HH. Thiocyanate levels in human saliva: quantitation by Fourier transform infrared spectroscopy. Anal Biochem. 1996;240(1):7–12. [PubMed: 8811872]
15. Gerson C, Sabater J, Scuri M, Torbati A, Coffey R, Abraham JW, et al. The lactoperoxidase system functions in bacterial clearance of airways. Am J Respir Cell Mol Biol. 2000;22(6):665–71. [PubMed: 10837362]
16. Gould NS, Gauthier S, Kariya CT, Min E, Huang J, Day BJ. Hypertonic saline increases lung epithelial lining fluid glutathione and thiocyanate: two protective CFTR-dependent thiols against oxidative injury. Respir Res. 2010;11:119. [PubMed: 20799947]
17. Minarowski L, Sands D, Minarowska A, Karwowska A, Sulewska A, Gacko M, et al. Thiocyanate concentration in saliva of cystic fibrosis patients. Folia Histochem Cytobiol. 2008;46(2):245–6. [PubMed: 18519245]
18. Skaff O, Pattison DI, Morgan PE, Bachana R, Jain VK, Priyadarsini KI, et al. Selenium-containing amino acids are targets for myeloperoxidase-derived hypothiocyanous acid: determination of absolute rate constants and implications for biological damage. Biochem J. 2012;441(1):305–16. [PubMed: 21892922]
19. Majerus PM, Courtois PA. Susceptibility of Candida albicans to peroxidase-catalyzed oxidation products of thiocyanate, iodide and bromide. J Biol Buccale. 1992;20(4):241–5. [PubMed: 1306188]
20. Mikola H, Waris M, Tenovuo J. Inhibition of herpes simplex virus type 1, respiratory syncytial virus and echovirus type 11 by peroxidase-generated hypothiocyanite. Antiviral Res. 1995;26(2):161–71. [PubMed: 7605114]
21. Pourtois M, Binet C, Van Tieghem N, Courtois P, Vandenabbeele A, Thiry L. Inhibition of HIV infectivity by lactoperoxidase-produced hypothiocyanite. J Biol Buccale. 1990;18(4):251–3. [PubMed: 2128884]
22. Chandler JD, Nichols DP, Nick JA, Hondal RJ, Day BJ. Selective metabolism of hypothiocyanous acid by mammalian thioredoxin reductase promotes lung innate immunity and antioxidant defense. J Biol Chem. 2013;288(25):18421–8. [PubMed: 23629660]
23. Caldwell KA, Tappel AL. Reactions of Seleno- and Sulfoamino Acids with Hydroperoxides. Biochemistry. 1964;3:1643–7. [PubMed: 14235323]

24. Eckenroth B, Harris K, Turanov AA, Gladyshev VN, Raines RT, Hondal RJ. Semisynthesis and characterization of mammalian thioredoxin reductase. Biochemistry. 2006;45(16):5158–70. [PubMed: 16618105]
25. Nagy P, Jameson GN, Winterbourn CC. Kinetics and mechanisms of the reaction of hypothiocyanous acid with 5-thio-2-nitrobenzoic acid and reduced glutathione. Chem Res Toxicol. 2009;22(11):1833–40. [PubMed: 19821602]
26. Eyer P, Worek F, Kiderlen D, Sinko G, Stuglin A, Simeon-Rudolf V, et al. Molar absorption coefficients for the reduced Ellman reagent: reassessment. Anal Biochem. 2003;312(2):224–7. [PubMed: 12531209]
27. Noble RW, Gibson QH. The reaction of ferrous horseradish peroxidase with hydrogen peroxide. J Biol Chem. 1970;245(9):2409–13. [PubMed: 5442280]
28. Ziegenhorn J, Senn M, Bucher T. Molar absorptivities of beta-NADH and beta-NADPH. Clin Chem. 1976;22(2):151–60. [PubMed: 2389]
29. Brechbuhl HM, Min E, Kariya C, Frederick B, Raben D, Day BJ. Select cyclopentenone prostaglandins trigger glutathione efflux and the role of ABCG2 transport. Free Radic Biol Med. 2009;47(6):722–30. [PubMed: 19520157]
30. Winterbourn CC. Comparative reactivities of various biological compounds with myeloperoxidase-hydrogen peroxide-chloride, and similarity of the oxidant to hypochlorite. Biochim Biophys Acta. 1985;840(2):204–10. [PubMed: 2986713]
31. Furtmuller PG, Zederbauer M, Jantschko W, Helm J, Bogner M, Jakopitsch C, et al. Active site structure and catalytic mechanisms of human peroxidases. Arch Biochem Biophys. 2006;445(2): 199–213. [PubMed: 16288970]
32. van Dalen CJ, Whitehouse MW, Winterbourn CC, Kettle AJ. Thiocyanate and chloride as competing substrates for myeloperoxidase. Biochem J. 1997;327 (Pt 2):487–92. [PubMed: 9359420]
33. Arner ES. Focus on mammalian thioredoxin reductases--important selenoproteins with versatile functions. Biochim Biophys Acta. 2009;1790(6):495–526. [PubMed: 19364476]
34. Rhee SG, Kil IS. Multiple Functions and Regulation of Mammalian Peroxiredoxins. Annu Rev Biochem. 2017;86:749–75. [PubMed: 28226215]
35. Torrents E Ribonucleotide reductases: essential enzymes for bacterial life. Front Cell Infect Microbiol. 2014;4:52. [PubMed: 24809024]
36. Torrents E, Aloy P, Gibert I, Rodriguez-Trelles F. Ribonucleotide reductases: divergent evolution of an ancient enzyme. J Mol Evol. 2002;55(2):138–52. [PubMed: 12107591]
37. Courtois PH, Pourtois M. Purification of NADH: hypothiocyanite oxidoreductase in Streptococcus sanguis. Biochem Mol Med. 1996;57(2):134–8. [PubMed: 8733891]
38. Barrett TJ, Pattison DI, Leonard SE, Carroll KS, Davies MJ, Hawkins CL. Inactivation of thiol-dependent enzymes by hypothiocyanous acid: role of sulfenyl thiocyanate and sulfenic acid intermediates. Free Radic Biol Med. 2012;52(6):1075–85. [PubMed: 22248862]

Highlights

- Selenocyanate ($^{-}$SeCN) is a biomimic of the endogenous anion thiocyanate ($^{-}$SCN).
- $^{-}$SeCN is utilized by lactoperoxidase and generates hyposelenocyanite (HOSeCN).
- HOSeCN is metabolized by the host but not the pathogen's thioredoxin reductase.
- HOSeCN is antimicrobial against many common cystic fibrosis (CF) lung pathogens.
- HOSeCN is effective against CF pathogens that are resistant to hypothiocyanate.

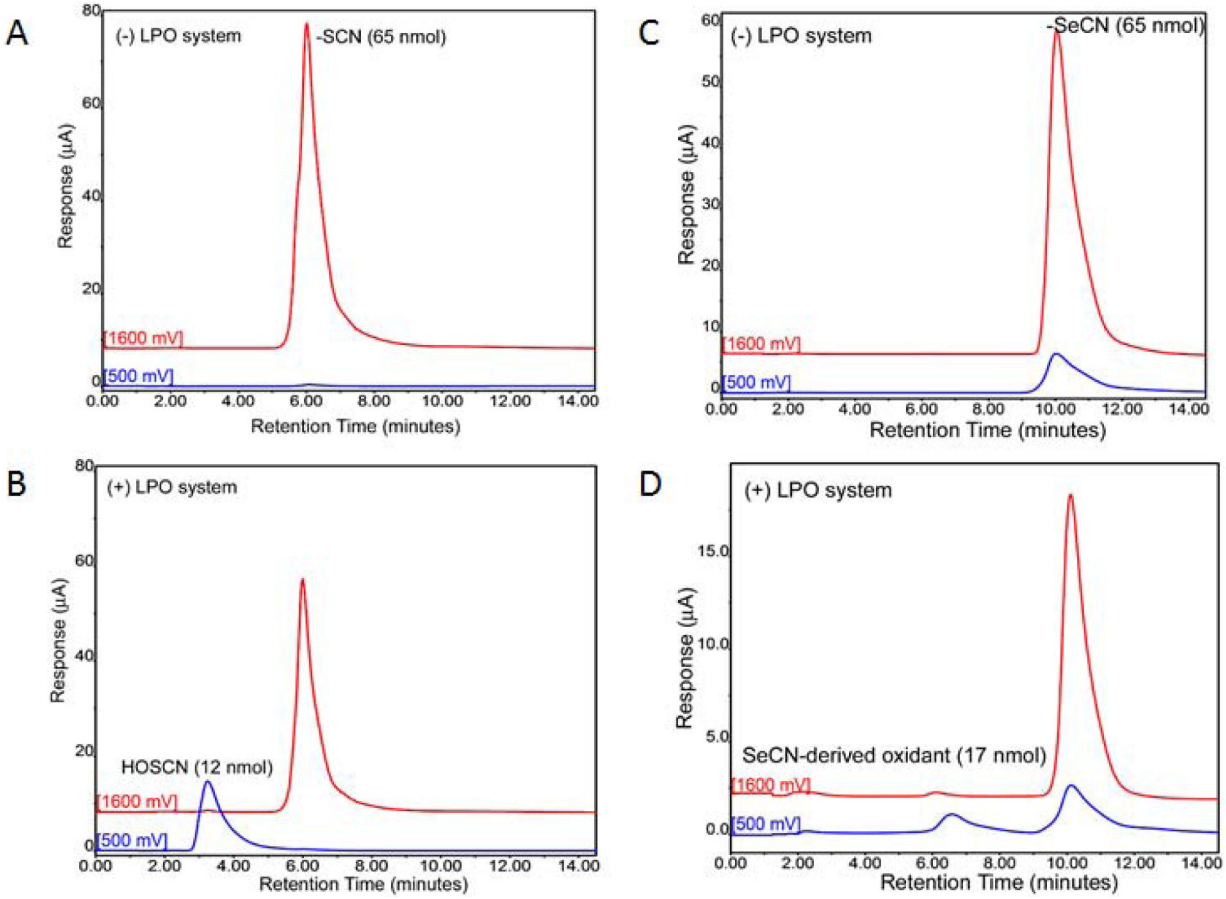

Figure 1.

Formation of oxidants from lactoperoxidase (LPO) system identified by HPLC with electrochemical detection (HPLC-EC). (A) Thiocyanate ($^{-}$SCN) detection by HPLC-EC at 1600 mV potential without the LPO system. (B) Loss of $^{-}$SCN signal at 1600 mV and formation of HOSCN signal at 500mV with LPO system. (C) Selenocyanate ($^{-}$SeCN) detection by HPLC-EC at both 1600 mV and 500 mV potentials without LPO system. (D) Loss of $^{-}$SeCN signal at both 1600 and 500 mV potentials and formation of oxidant signal at 500 mV with LPO system.

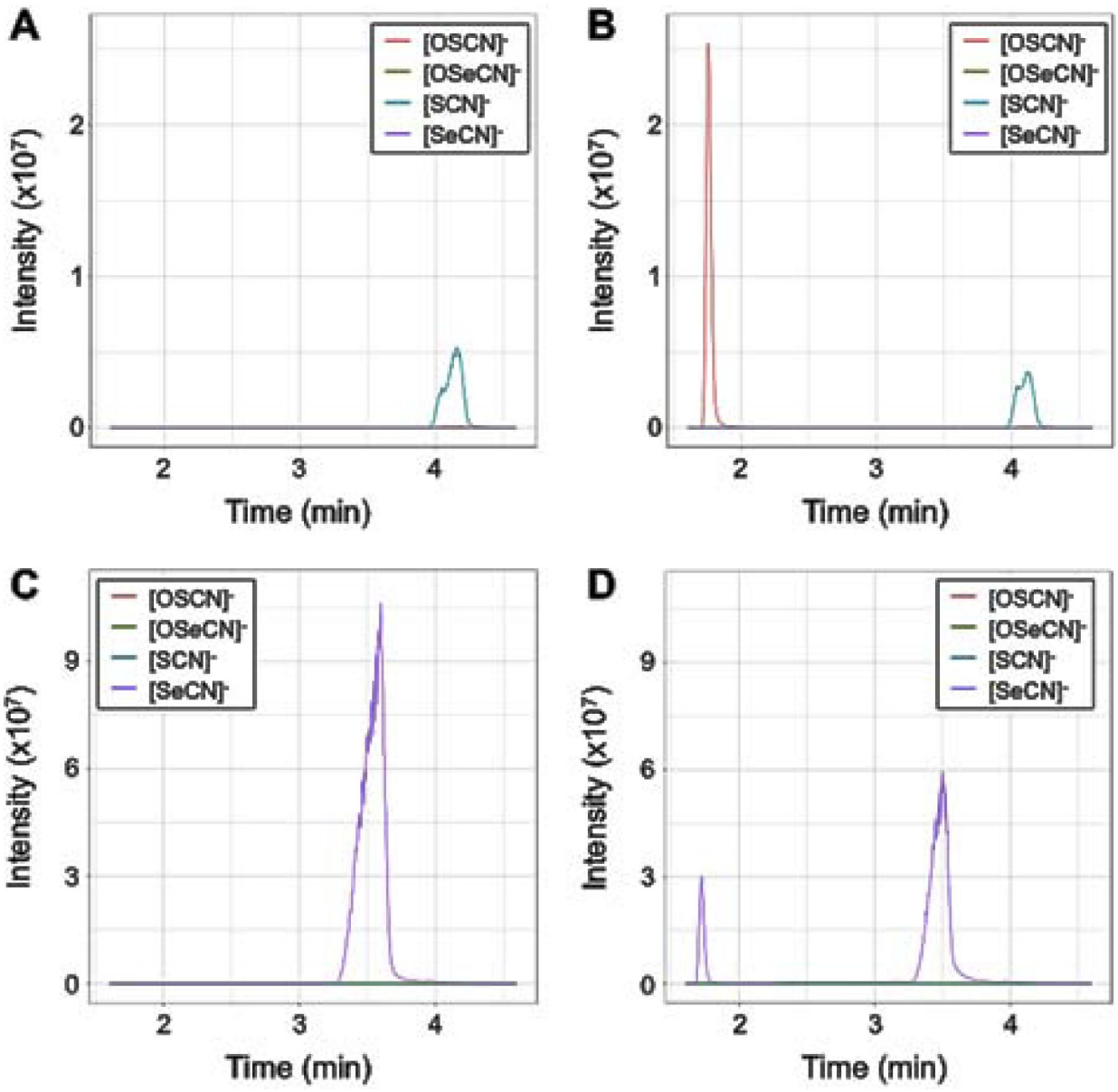

Figure 2. Characterization of LPO-catalyzed ⁻SeCN oxidation via mass spectrometry.

⁻SCN or ⁻SeCN was oxidized with LPO and hydrogen peroxide and the oxidant product was quantified with the TNB assay. The oxidant was then diluted to 10 μM in PBS and extracted for LC-MS. Negative controls with hydrogen peroxide replaced by water were diluted by an equal amount to the oxidant samples. We extracted high mass accuracy (5 ppm) ion chromatograms for the $[M-H]^-$ ions of our target compounds, which corresponded to $[SCN]^-$ (blue trace), $[OSCN]^-$ (red trace), $[SeCN]^-$ (purple trace) and $[OSeCN]^-$ (green trace). (A) ⁻SCN and LPO without addition of hydrogen peroxide. (B) ⁻SCN and LPO with addition of hydrogen peroxide. (C) ⁻SeCN and LPO without addition of hydrogen peroxide. (D) ⁻SeCN and LPO with addition of hydrogen peroxide.

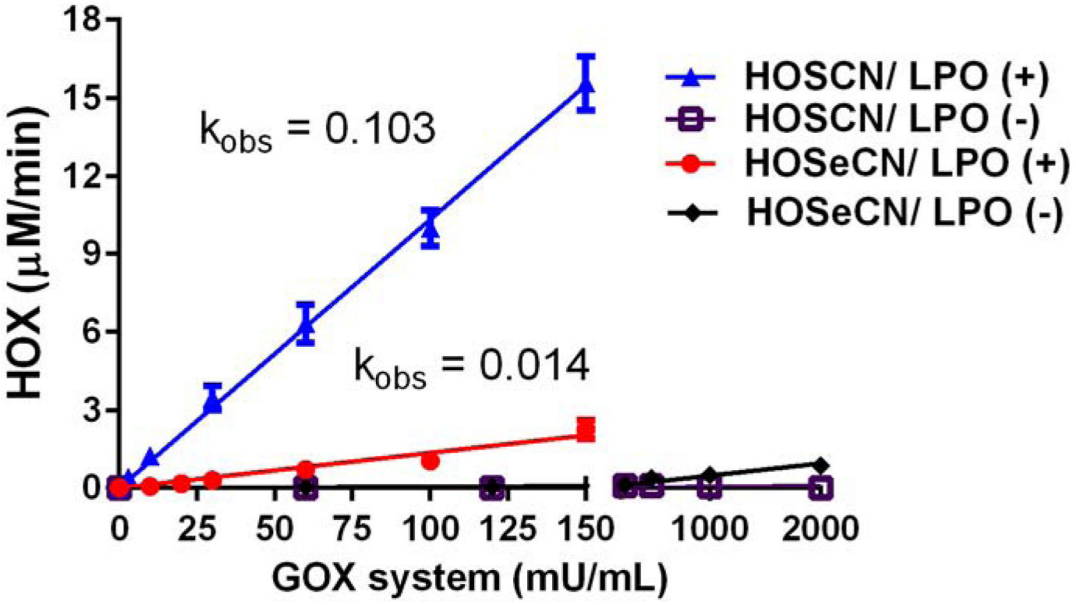

Figure 3.

Generation of oxidants (HOX) from LPO system using ⁻SCN or ⁻SeCN as substrates. LPO oxidant formation using ⁻SCN (triangles) or ⁻SeCN (circles) as substrates was followed spectrophotometrically by oxidation of NTB to DNTB at 412 nm over 2 minutes. Non-enzymatic formation (minus LPO) of oxidants with ⁻SCN (squares) or ⁻SeCN (diamonds) was also assessed. Rates of HOX determined from linear regression of 4 replicates per glucose oxidase (GOX) concentration. HOSCN production was 0.103 μM/mU/mL GOX and HOSeCN production was 0.014 μM/mU/mL GOX.

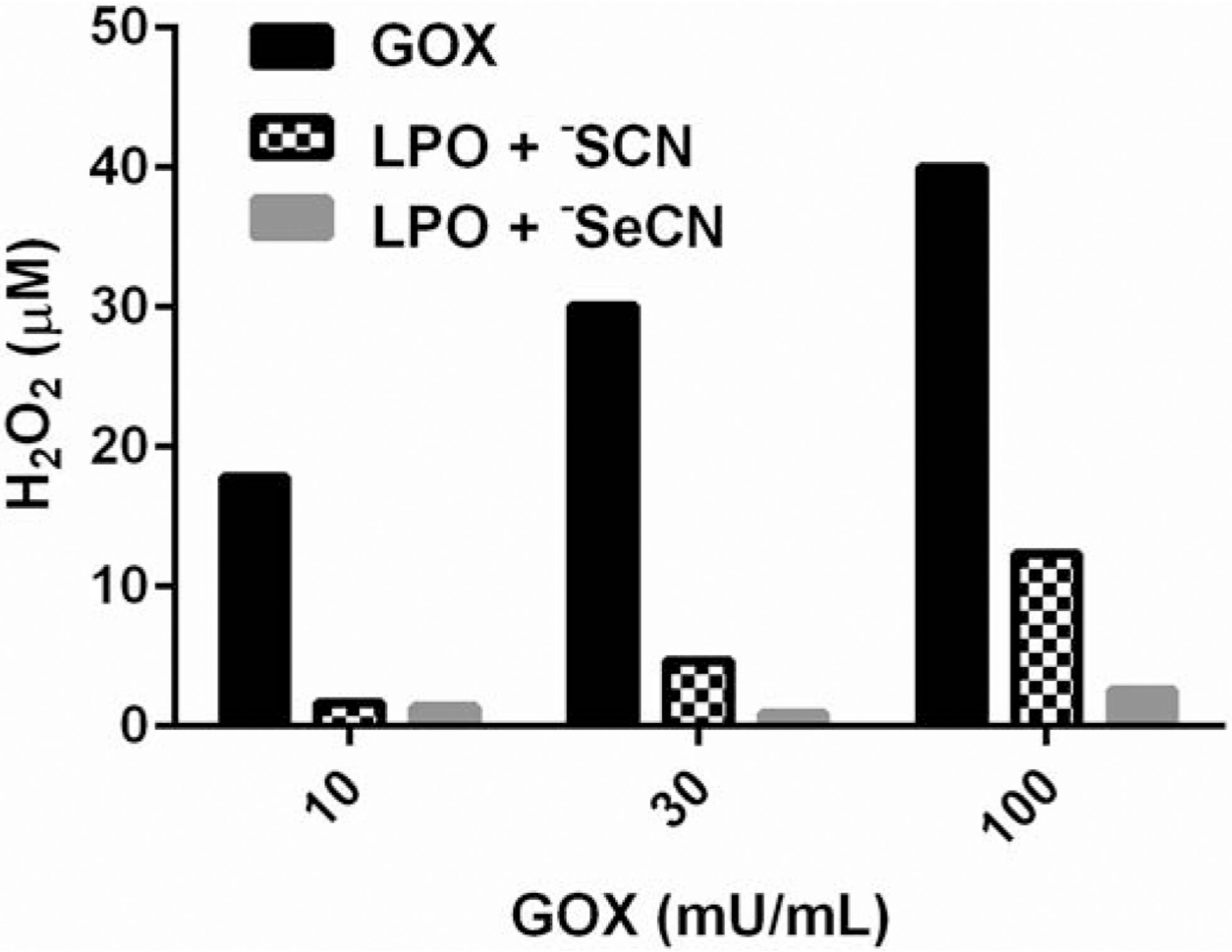

Figure 4.

Residual hydrogen peroxide levels in the presence and absence of the full system of LPO, glucose oxidase (GOX) and ¯SCN or ¯SeCN after a 2-hour incubation at room temperature. Hydrogen peroxide levels were determined using a calibrated hydrogen peroxide electrode. Black bars are hydrogen peroxide levels with GOX system only, hatched bars are the LPO system plus ¯SCN (1 mM), and grey bars are the LPO system with ¯SeCN (1 mM).

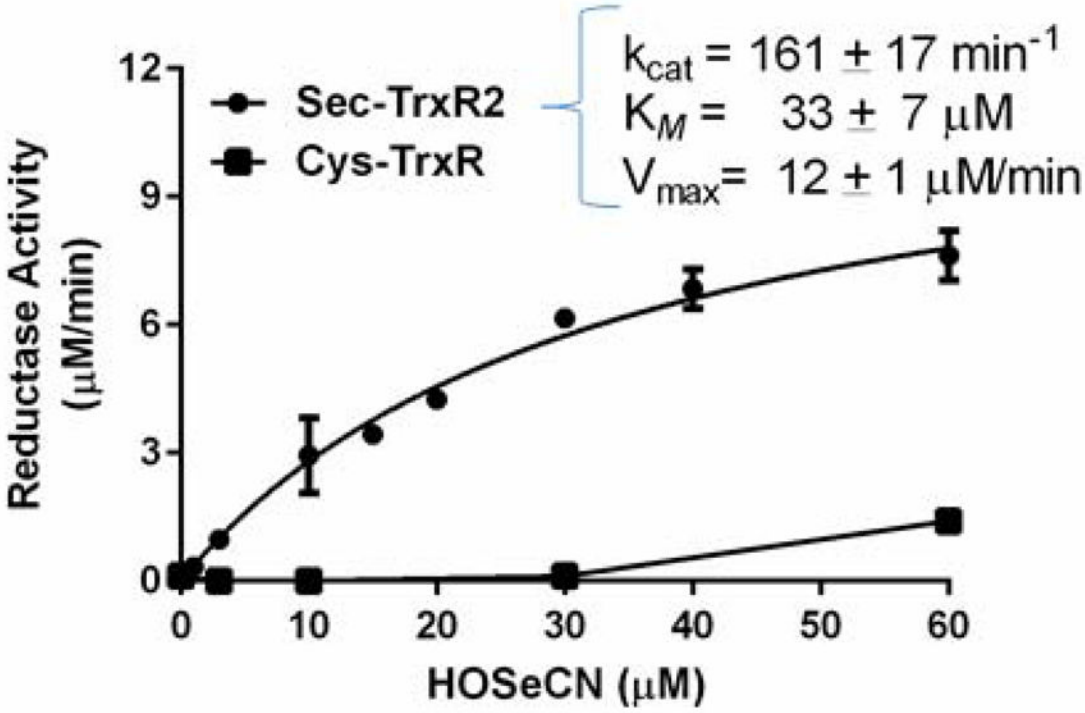

Figure 5.

Kinetic analysis of HOSeCN metabolism by recombinant mouse Sec-TrxR2 and recombinant *E. coli.* Cys-TrxR. Activity was measured spectrophotometrically as substrate dependent NADPH consumption at 340 nm. Mammalian Sec-containing TrxR can readily metabolize HOSeCN with a *Km* of 33 μM, Vmax of 12 μM/min, and kcat of 161 min^{-1} (circles) whereas there was only measurable activity high HOSeCN levels with the *E. coli* form of Cys-TrxR (squares).

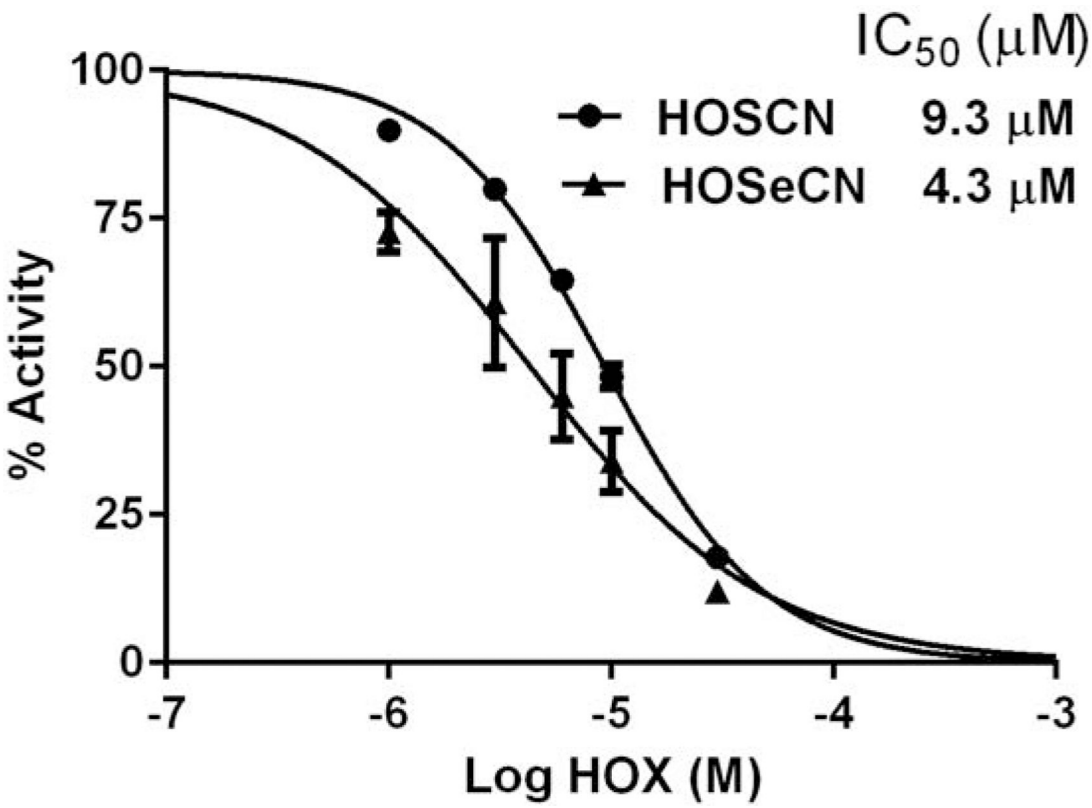

Figure 6.

Comparison of HOSCN and HOSeCN inhibition of bacterial Cys-TrxR. *E. coli* recombinant Cys-TrxR was incubated with increasing concentrations of either HOSCN (circles) or HOSeCN (triangles) for 5 minutes before addition of *E. coli* Trx. Activity was measured spectrophotometrically as substrate-dependent NADPH consumption at 340 nm. HOSeCN was slightly more potent inhibitor of bacterial Cys-TrxR with an IC_{50} of 4.3 μM as compared to HOSCN IC_{50} of 9.3 μM.

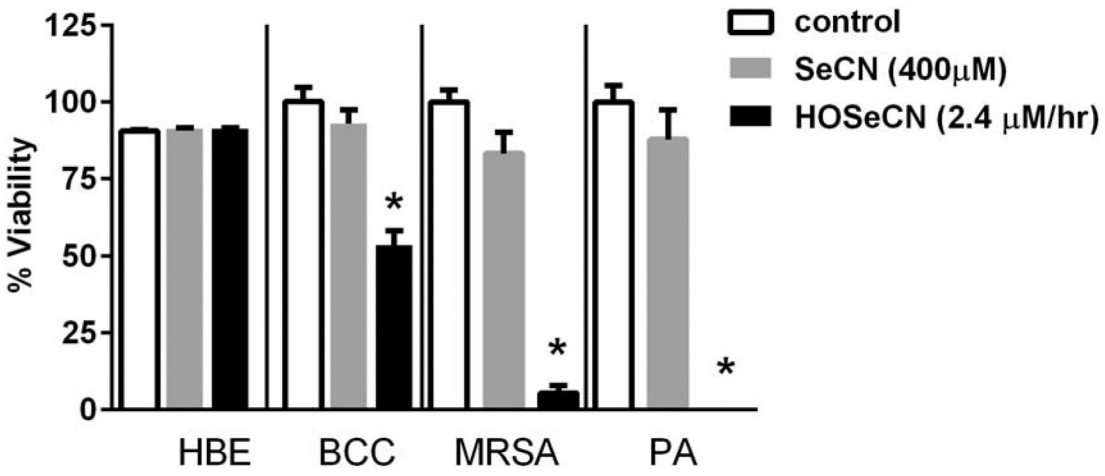

Figure 7.

HOSeCN generation spares host lung epithelial cells while killing bacteria. Human bronchial epithelial cells (HBE) or bacteria (*Burkholderia multivorans* (BCC), methicillin resistant *Staphylococcus aureus* (MRSA), *Pseudomonas aeruginosa* (PA)) were treated for 2 hour in PBS (control), SeCN only (grey bar) or full peroxidase system (black bar) at pH 7.4 and then media replaced and viability assessed 24 hours later. HBE cell viability assessed by LDH assay and bacterial cell viability assessed by colony forming units. *$p<0.05$ versus control.

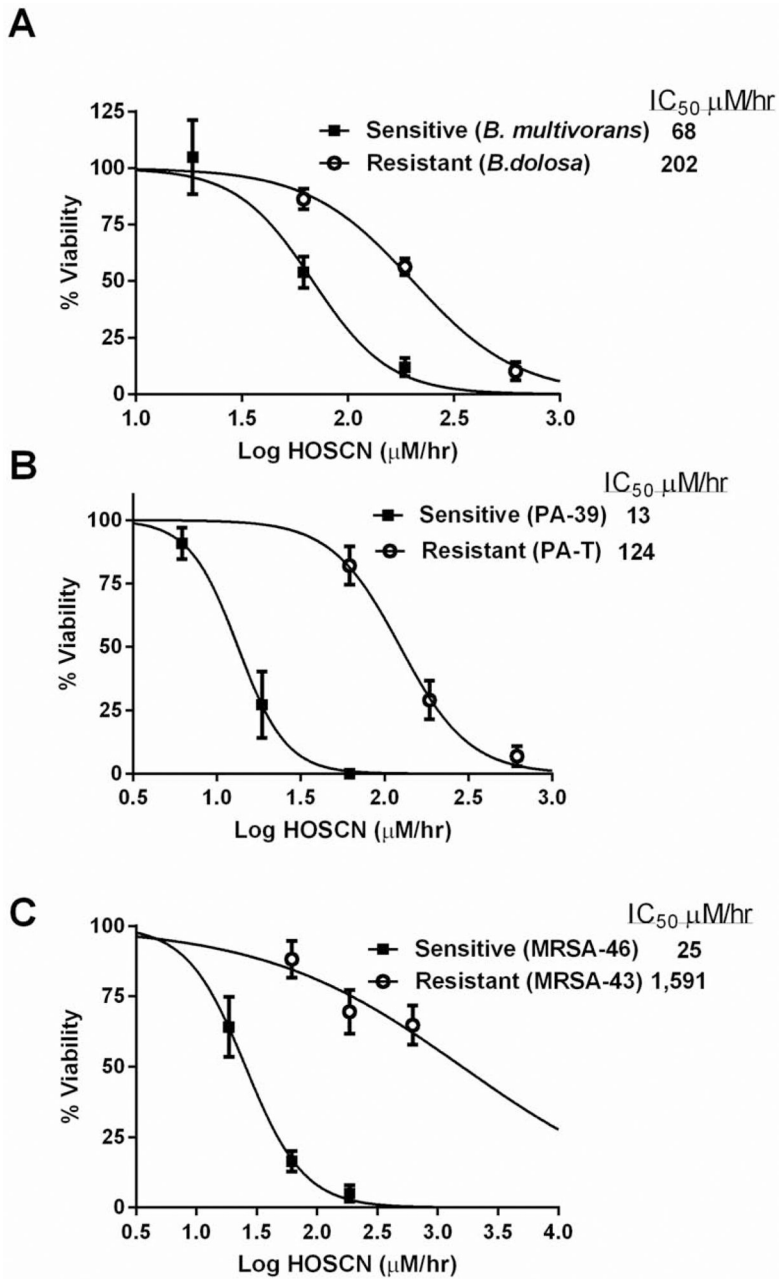

Figure 8.

Hypothiocyanite (HOSCN) resistance in CF relevant bacterial isolates. Comparison of a HOSCN resistant (open circles) and sensitive (closed squares) **(A)** BCC clinical isolate, **(B)** PA clinical isolate, and **(C)** MRSA clinical isolate. Bacteria cell viability assessed 24 hours after a 2-hour exposure to HOSCN generating system with viability assessed by CFUs. The flux of either HOSCN or HOSeCN (HOX) was determined from rates determined in Figure 3. LC_{50} values were determined by curve fitting the data with nonlinear regression of log (agonist) vs normalized response.

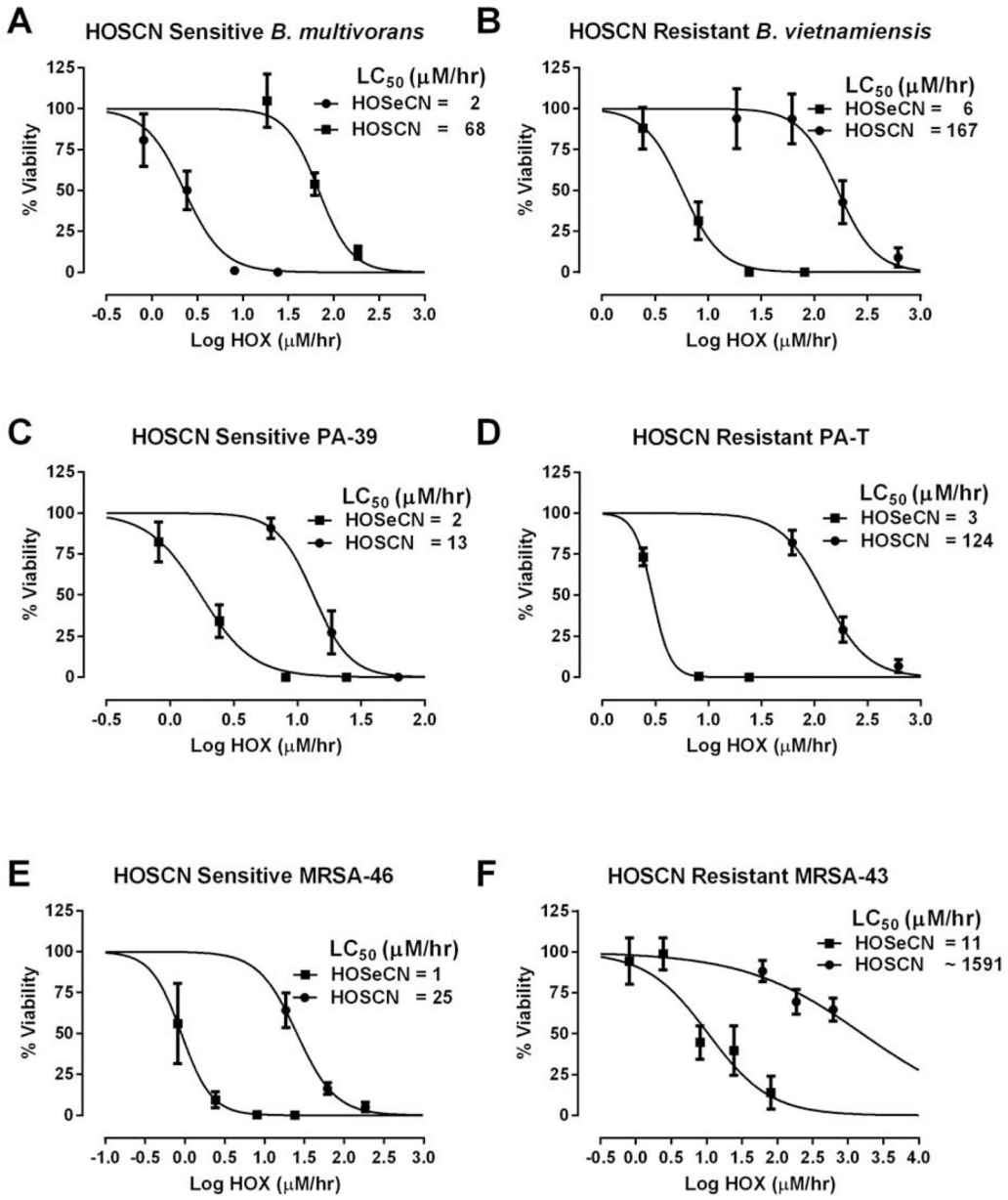

Figure 9.

Comparison of bacterial killing between $^{-}$SCN/HOSCN and $^{-}$SeCN/HOSeCN systems in $^{-}$SCN sensitive and resistant bacterial strains. Comparisons of HOSCN sensitive (circles) and resistant (squares) strains of BCC clinical isolates (A&B), PA clinical isolates (C&D), and MRSA clinical isolates (E&F). Bacteria were incubated for 2 hours with LPO, $^{-}$SCN or $^{-}$SeCN, glucose and increasing amounts of glucose oxidase. The flux of either HOSCN or HOSeCN (HOX) was determined from rates determined in Figure 3. LC_{50} values were determined by curve fitting the data with nonlinear regression of log (agonist) vs normalized response.

Table 1.

Bacterial sensitivity towards HOSCN killing

Bacterial Strains	**HOSCN IC_{50} (μM/hr)**	**95% CI (μM/hr)**
Burkholderia cepacia complex (BCC)		
B. multivoran *	68	52-91
B. cenocepacia *	151	111-206
B. vietnamiensis *	167	103-207
B. dolosa *	202	167-245
Pseudomonas aeruginosa (PA)		
PA-39 *	13	10-18
PA-X *	33	23-47
PAO1	34	24-48
PA-AMT-105 *	42	26-67
PA-N3 *	80	62-104
PA-K4 *	90	59-137
PA-T *	124	96-161
Methicillin resistant *Staphylococcus aureus* (MRSA)		
46 *	25	19-34
45 *	40	26-62
44 *	707	357-1,391
43 *	1,591	201-12,618

* Isolates from CF sputum